*4th URSI AT-RASC, Gran Canaria, 19-24 May 2024*

# Magneto-dielectric Microstrip Antennas on 3D-Printed Substrates with Selectively Deposited Magnetic Regions

Jakub Sorocki(1), Constantine Kakoyiannis(2), and Ilona Piekarz(1)
(1) Institute of Electronics, AGH University of Science and Technology, Krakow, Poland
(2) Antennas & EM Modelling Department, IMST GmbH, Kamp-Lintfort, Germany

## Abstract

Microstrip antennas on 3D-printed magneto-dielectric substrates with selectively deposited magnetic regions are presented. Low-cost fused filament fabrication was used together with COTS dielectric and ferromagneto-dielectric filaments. Eight patch antennas operating within 0.9–1.2 GHz were built and experimentally studied. Apart from two uniform, reference substrates, others were loaded with magnetic regions of different shapes or thicknesses. We studied the effect of loading on the radiation efficiency and Q-factor of the antennas while monitoring the miniaturization degree offered by the magnetic profiles. Our findings indicate that the magnetic profile significantly affects all three metrics. Additive manufacturing is a key enabler of selective material deposition, which is a prerequisite of magnetic profiling. Although the method described herein holds promise, the high losses of iron-doped filaments make the shift toward ferri-magnetic (ceramic) fillers rather necessary.

## 1. Introduction

Constant advances in wireless communication increase the demand for low-cost, low-profile, highly efficient, compact antennas; this is the case for the popular microstrip antenna [1]. One technique to miniaturize microstrip antennas is high-permittivity (high-$\varepsilon_r$) substrates, however, this reduces both antenna efficiency, $\eta_{rad}$, and bandwidth (BW), because an increase in $\varepsilon_r$ of a non-permeable substrate causes a reduction in intrinsic wave impedance.

MD materials feature a permeability above unity ($\mu_r > 1$) and can be used to load the substrates of patch antennas [2]–[7]. An advantage of MD antennas (MDAs) is that they can offer increased bandwidth at a constant electrical size or maintain bandwidth at reduced electrical size [2], [3]; they are also frequency & polarization reconfigurable [5]. Apart from size & BW improvements, maintaining high efficiency is yet another important issue in antenna design. When magnetic loss tangent is reasonably low (on the order of FR4 loss), it is possible to obtain 50–80% efficient antennas [2], [3], [7]. When magnetic loss dominates, the result is $\eta_{rad} < 10\%$ [4], [7].

A promising approach to the realization of MDAs is 3D printing technology since it combines rapid and low-cost fabrication with high design flexibility. In [6]–[7], a COTS polylactic acid (PLA) polymer doped with ferromagnetic filler (iron particles) was used to realize the entire substrate of patch antennas at 1 GHz and 0.6 GHz, respectively. The results in [7] showed that, for thick magneto-dielectric substrates with optimized ground plane sizes, efficiencies on the order of 50% are possible in a narrow band, even though the iron-doped filament exhibited relatively high magnetic losses.

Contrary to [6]–[7], this paper focuses on 3D-printed MD substrates with selectively deposited magnetic regions, as a way to mitigate magnetic losses, while making antennas electrically smaller and achieving a wave impedance closer to that of free space (377 Ω). Magnetic profiles and locations were selected aiming for the strong magnetic field along the non-radiating edges of the patch. Eight probe-fed, square patch antennas operating in the 0.9–1.2 GHz range were built by fused filament fabrication (FFF). Except for two uniform reference substrates, the other six substrates were loaded with different magnetic profiles. We studied the effect of the MD loadings on $\eta_{rad}$ and Q-factor of the eight antennas while monitoring the achieved miniaturization degree.

## 2. Antenna Fabrication

To perform the analysis on the influence of the MD profile deposited in the substrate, a set of eight patch antennas was designed and realized using additive manufacturing. The presented approach exploits the concept presented in 0–0, where the magneto-dielectric material constituted the patch antenna substrate in its entirety, and the influence of substrate thickness was investigated. In the present work, all the antennas were designed to have the same:

- patch size equal to 80 mm × 80 mm,
- ground plane size equal to 120 mm × 120 mm,
- substrate thickness equal to 3 mm,
- probe feeding point 10 mm from patch edge.

*A. Substrates with selectively deposited magnetic regions*

We began by building two reference antennas, herein termed “ANT0” and “ANT1”. ANT0 is not magnetically loaded; its substrate is purely dielectric. The substrate of ANT1, on the other hand, is completely MD in all three dimensions, as in 0–0. Then, we moved on to build ANT2, which is a hybrid of the previous two; the MD material covers the entire horizontal plane but only half the thickness (1.5 mm out of 3 mm); the rest of the thickness towards the ground plane was filled with a purely dielectric material.

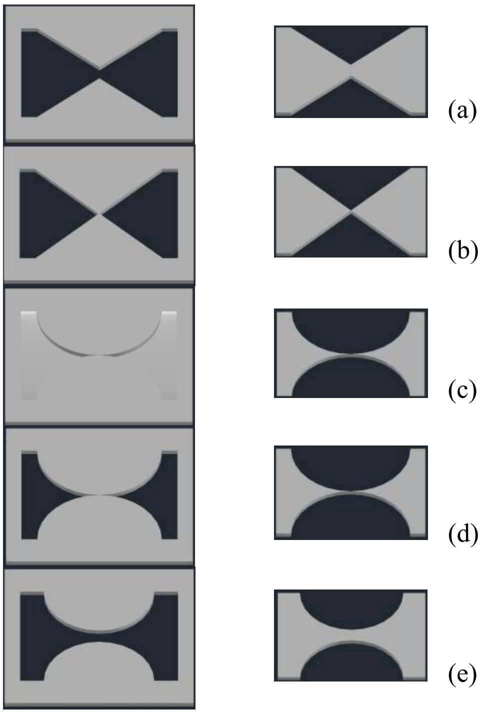

**Figure 1.** Variation of magneto-dielectric material profile (right) deposited in a dielectric substrate (left) for investigation of patch antenna efficiency: (a) ANT3, (b) ANT4, (c) ANT5, (d) ANT6, (e) ANT7.

**Table 1.** Microstrip AUTs with selectively deposited magnetic regions of varying profile in areas of strong magnetic field. Each AUT is an 80 mm × 80 mm probe-fed patch on a 120 mm × 120 mm × 3 mm substrate.

| Unit | Embed. profile | Prof. width @ centr. ax. | Thickness | Frac. volume* |
|---|---|---|---|---|
| ANT0 | none | - | - | |
| ANT1 | full plane | - | host | 100 % |
| ANT2 | full plane | - | half host under patch | 50 % |
| ANT3 | linear taper | 0 mm | host | 50 % |
| ANT4 | linear taper | 10 mm | host | 56.3% |
| ANT5 | elliptical taper | 0 mm | ellipt. taper | 15% |
| ANT6 | elliptical taper | 0 mm | host | 21.5% |
| ANT7 | elliptical taper | 10 mm | host | 39.3% |

*Magnetic material volume under the patch as a fraction of the total volume under the patch.

Microstrip antennas have independent radiation and resonance mechanisms; the patch resonates from the currents flowing along its length, but it radiates from the **E**-field along the two radiating edges. Therefore, it can be argued that a bow-tie–shaped MD region embedded in a dielectric substrate might be the best solution to improve the efficiency and reduce the electrical size of a microstrip antenna. In any case, the selectively deposited MD profile must be subjected to optimization. To investigate several possibilities, we built the five variations of the bow-tie MD profile shown in Fig. 1, denoted as ANT3–ANT7. A summary of the geometry of each antenna-under-test (AUT) is given in Table 1.

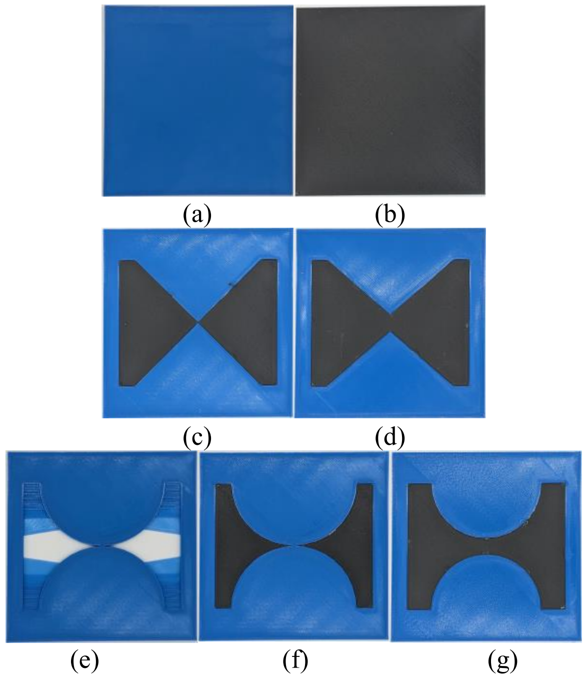

**Figure 2.** Photographs of the fabricated substrates (patch side view): (a) ANT0, (b) ANT1/2, (c) ANT3, (d) ANT4, (e) ANT5 (magnetic insert removed for clarity), (f) ANT6, and (g) ANT7.

*B. Substrate 3D printing and AUT assembly*

The substrates were 3D printed using FFF technology; two commercially available filaments were utilized, i.e., blue PLA 1.75 mm filament from Amazon Basics (herein termed "PLA") 0 and magnetic iron PLA 1.75 mm filament from Proto-pasta (herein termed "FePLA") 0. The latter is a low-cost iron-doped PLA material exhibiting $\varepsilon_r$, $\mu_r > 1$. An Original Prusa i3 MK3 3D printer by Prusa Research was used with the .gcode generated by the PrusaSlicer software. The digital 3D models of every antenna substrate (pure PLA and iron-doped PLA) were sliced into 12 layers, each 0.25 mm thick, to produce substrates of the targeted thickness. Additionally, a solid infill being 100% rectilinear at 45° was used for all layers with infill extrusion width at 0.45 mm for maximum printed trace density [10]. Both pure PLA and FePLA materials were printed using a 0.4 mm nozzle hardened for matched printing settings. Due to the relatively small print volume of the insert, no larger nozzle was required for FePLA, even though the iron content causes the material to be more abrasive, brittle, and prone to clogging. As a result, FePLA required greater attention during printing. Manufacturing of the substrates was carried out at the extrusion temperature of $T_{ext}$ = 215 °C (a setting below the Curie temperature of iron, hence the ferromagnetic behavior was maintained), heated bed temperature of $T_{bed}$ = 60 °C, and cooling of 100% after the first layer.

At first, test substrates were 3D printed; one out of PLA and the other out of FePLA filament, to characterize material properties as in 0. At 1 GHz, PLA material properties are $\varepsilon_r = 2.65$, $\tan\delta_\varepsilon = 0.01$, whereas FePLA properties are $\varepsilon_r = 3.49$, $\tan\delta_\varepsilon = 0.01$, $\mu_r = 1.22$, $\tan\delta_\mu = 0.17$. The magnetic losses of FePLA are more than an order of magnitude higher than the dielectric losses. The interested reader may find a discussion on the sources of magnetic loss in iron-doped PLA in 0.

(a)

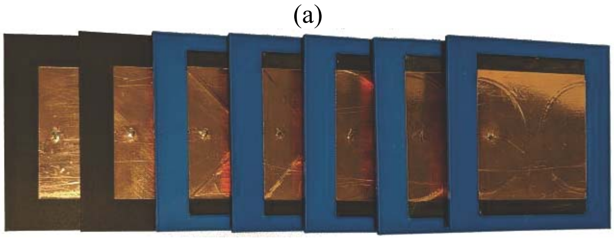

(b)

**Figure 3.** (a) A photograph of a fully assembled AUT (top and bottom view), and (b) antenna set. Magnetic regions extend 10 mm past the non-radiating edges, whereas probe feed is in the PLA region, 10 mm from the edge along the central axis.

The next step was to 3D-print the patch antenna substrates. All-dielectric and all-MD substrates for ANT0 and ANT1 were manufactured in a single-run process. The substrates for ANT2–ANT7, which are composed of two material types, were manufactured in a two-step process, i.e., the PLA and FePLA parts were printed separately due to a lack of multi-material extrusion. Next, the dielectric and MD parts were assembled and glued using epoxy. Photographs of the 3D-printed substrates are shown in Fig. 2. Then, the top and bottom metal layers were fabricated. Square patches were cut out of 25 µm–thick copper tape with adhesive backing and were attached on top of the substrates; the ground plane was realized similarly on the bottom side. Skin depth in copper at 1 GHz is roughly 2 µm, which means the copper tape is 8 times thicker. Finally, the stack-ups were drilled at the feeding point and SMA connectors were soldered. A photograph of the manufactured antenna set is shown in Fig. 3.

## 3. Experimental Results

All measurements were performed on the R&S ZND 2-port VNA in the 0.5–1.5 GHz band (201 points). The FS reflection coefficient at the input to the eight AUTs is shown in Fig. 4. Our focus was not on impedance matching, but rather on the efficiency and quality factor. Frequencies $f_0 = \mathrm{argmin}\{|S_{11}|\}$ lie in the range 0.91–1.16 GHz. Since the eight antennas have identical physical apertures, the miniaturization factor of antennas ANT1–7 w.r.t. ANT0 is simply the ratio of frequencies $m = f_{0,i} / f_{0,0}$, $i \in \{1, 2, \ldots, 7\}$. This is tabulated in Table 2, which shows that the all-FePLA ANT1 reduced its electrical size by 21.2% ($m$ = 0.788).

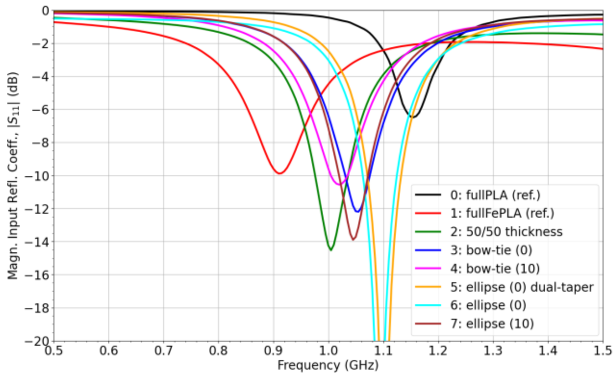


**Figure 4**. Magnitude of reflection coefficient at the input to the eight AUTs.

**Table 2**. Comparison of measured data across the eight fabricated AUTs.

| AUT | $f_0$ (GHz) | $m$ | $\eta_{rad}$ | $Q_A$ | FoM |
|---|---|---|---|---|---|
| ANT0 | 1.155 | 1.000 | 0.700 | 35.8 | 51.1 |
| ANT1 | 0.910 | 0.788 | 0.083 | 4.25 | 40.3 |
| ANT2 | 1.005 | 0.870 | 0.141 | 7.04 | 43.4 |
| ANT3 | 1.055 | 0.913 | 0.129 | 7.15 | 50.6 |
| ANT4 | 1.020 | 0.883 | 0.127 | 5.65 | 39.3 |
| ANT5 | 1.100 | 0.952 | 0.220 | 11.5 | 49.8 |
| ANT6 | 1.095 | 0.948 | 0.201 | 11.2 | 52.8 |
| ANT7 | 1.045 | 0.905 | 0.141 | 7.78 | 49.9 |

The efficiency of the five MDAs was measured employing the Wheeler Cap, which calculates efficiency indirectly by comparing the complex reflection coefficient at the input to the AUT in two different states, i.e., radiating in free space and placed inside a Faraday shield (cap) to choke radiation. Efficiency can be thus measured regardless of input matching, in a broad bandwidth and with arbitrary frequency resolution. Post-processing of the raw VNA data was done through the Improved Wheeler Cap (IWC) described in 0. Since the matching levels of the eight antennas differ, a comparison in terms of total efficiency, $\eta_T$, would not make sense; hence we focused on radiation efficiency. The full-band result is shown in Fig. 5. The uncertainty is $\Delta\eta_{rad} = \pm 0.02$. The all-PLA reference ANT0 is a 70% efficient antenna in the vicinity of its $f_0$. Similarly, the other seven antennas exhibit efficiencies in the range of 8–22%; the values of $\eta_{rad}$ at $f_0$ are listed in Table 2. As expected, MDA efficiency is inversely related to the fractional volume of iron-doped PLA under the patch. Quality factors, $Q_A$, were calculated from measured S-parameters according to 0; the broadband result is shown in Fig. 6, whereas $Q_A$-values at $f_0$ are listed in Table 2.

Magnetic loading reduces the $Q$-factor from 36 to values as low as 4; as expected 0, 0, 0, the potential of microstrip antennas for a wide BW can be greatly enhanced.

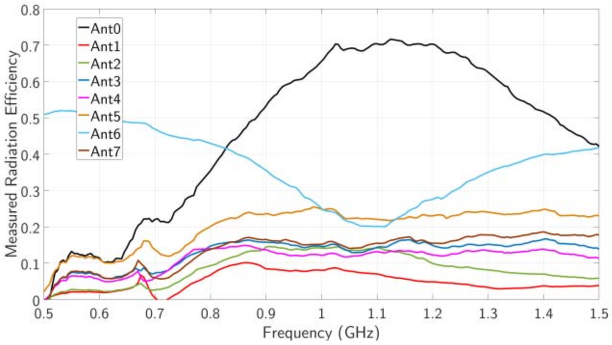


**Figure 5**. Measured radiation efficiency of the 8-antenna test set.

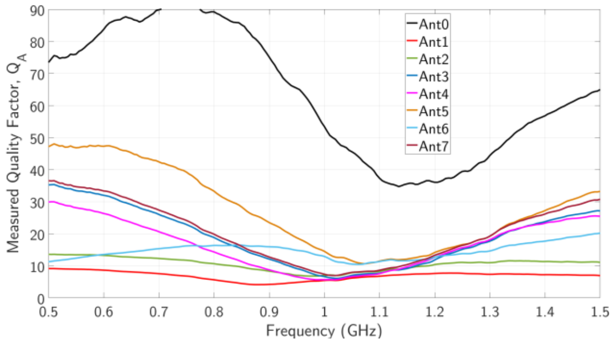


**Figure 6**. Measured $Q$-factor of the 8-antenna test set.

The right-most column in Table 2 is a figure-of-merit (FoM) that considers miniaturization factors, efficiency levels, and $Q_A$-values with equal weights; FoM = $(Q_A/\eta_{rad})\cdot m$; the lower the FoM, the better the *overall* antenna performance is. Variations in FoM across the eight AUTs are not that big (39–53). The results have been essentially masked by the magnetic losses of the FePLA inserts. For example, ANT4 (linear bow-tie profile) scores the best FoM due to its excellent $Q$-factor; however, it can be argued that a 13% efficiency is too low to satisfy a given link budget.

## 4. Conclusion

The findings presented in Section III indicate that the magnetic profile can affect all three metrics $m$, $\eta_{rad}$, and $Q_A$. However, high magnetic losses are detrimental to antenna performance, whereas magnetic profiles need to be kept away from the radiating edges of the patch by a few millimeters; profile optimization needs to include this distance. Additive manufacturing is a key enabler of selective material deposition, which is a prerequisite of optimum magnetic loading. Although the method described herein holds promise, the low $\mu_r$ and high $\tan\delta_\mu$ values of iron-doped filaments necessitate a shift towards ferri-magnetic (ceramic) composite materials. All the above are parts of ongoing research.

## 5. Acknowledgements


This research was funded by the National Science Centre, Poland, under Grant no. 2019/34/E/ST7/00342.


## References


[1] D. R. Jackson, "Microstrip antennas," in *Antenna Engineering Handbook*, 4th ed. J. L. Volakis, Ed. New York: McGraw-Hill, 2007, ch. 7.

[2] P. M. T. Ikonen, *et al.*, "Magneto-dielectric substrates in antenna miniaturization: Potential and limitations," *IEEE Trans. Antennas Propag.*, vol. 54, no. 11, pp. 3391–3399, Nov. 2006.

[3] A.O. Karilainen, *et al.*, "Experimental studies on antenna miniaturisation using magneto-dielectric materials," *IET Microw. Antennas Propag.*, vol. 5, no. 4, pp. 495–502, Apr. 2011.

[4] M. Aldrigo, *et al.*, "Numerical and experimental characterization of a button-shaped miniaturized UHF antenna on magneto-dielectric substrate," *Int. J. Microw. Wireless Technologies*, vol. 5, no. 3, pp. 231–239, Jun. 2013.

[5] E. Andreou, *et al.*, "Magneto-dielectric materials in antenna design: Exploring the potentials for reconfigurability," *IEEE Antennas Propag. Mag.*, vol. 61, no. 1, pp. 29–40, Feb. 2019.

[6] J. Sorocki, *et al.*, "Realization of compact patch antennas on magneto-dielectric substrate using 3D printing technology with iron-enhanced PLA filament," in *Proc. Int'l Conf. Electromagn. Advanced Appl.*, Cartagena de Indias, Colombia, 2018.

[7] C. Kakoyiannis, *et al.*, "Microstrip antennas on 3D-printed magneto-dielectric substrates: Fabrication and efficiency study," *Int. J. Microw. Wirel. Technol.*, early access, 2023.

[8] Amazon Basics, *3D Printer filament Data Sheet*.

[9] Proto-pasta, *Magnetic Iron PLA Data Sheet*.

[10] V. E. Kuznetsov, *et al.*, "Strength of PLA components fabricated with fused deposition technology using a desktop 3D printer as a function of geometrical parameters of the process," *MDPI Polymers*, vol. 10, no. 3, 313, 2018.

[11] J. Sorocki, *et al.,* "Broadband permittivity and permeability extraction of 3-D printed magneto-dielectric substrates," *IEEE Microw. Wirel. Compon. Lett.*, no. 10, pp. 1174-1177, Oct. 2021.

[12] C. G. Kakoyiannis, "Post-processing accuracy enhancement of the improved Wheeler cap for wideband antenna efficiency measurements," in *Proc. 8th Eur. Conf. Antennas Propag.*, The Hague, The Netherlands, 2014, pp. 342–346.

[13] A. D. Yaghjian, "Improved formulas for the Q of antennas with highly lossy dispersive materials," *IEEE Antennas Wireless Propag. Lett.*, vol. 5, pp. 365–369, 2006.